VILNIUS UNIVERSITY

CPST PHYSICS INSTITUTE

Paulius Každailis

LEAKY ACOUSTIC WAVES IN ACOUSTO-OPTIC AND ACOUSTO-ELECTRIC INTERACTION

PhD thesis summary

Physical sciences, Physics (02 P)

Vilnius, 2012

The thesis was prepared at Vilnius University in 2006-2011.

Scientific superviser:
- Prof. habil. dr. Daumantas Čiplys (Vilnius University, Physical sciences, Physics – 02 P).

Adviser:
- Doc. dr. Romualdas Rimeika (Vilnius University, Physical sciences, Physics – 02 P).

The thesis will be defended at the council of Physics science direction at Vilnius University:

Chairman:
- Prof. habil. dr. Gintautas Tamulaitis (Vilnius University, Physical sciences, Physics – 02 P);

Members:
- Prof. habil. dr. Alfonsas Grigonis (Kaunas University of Technology, Physical sciences, Physics – 02 P);
- Dr. Rimantas Miškinis (Semiconductor Physics Institute of Center for Physical Sciences and Technology, Physical sciences, Physics – 02 P).
- Prof. dr. Šarūnas Paulikas (Vilnius Gediminas Technical University, Technological sciences, Electrical and electronic engineering – 01 T);
- Doc. dr. Vytautas Samulionis (Vilnius University, Physical sciences, Physics – 02 P);

Opponents:
- Prof. habil. dr. Rymantas Kažys (Kaunas University of Technology, Technological sciences, Electrical and electronic engineering – 01 T);
- Doc. dr. Vytautas Kunigėlis (Vilnius University, Physical sciences, Physics – 02 P).

The thesis will be defended at the public meeting of the Physics science direction council on April 20th, 2012 at 3 p. m. in the 815 auditorium of the Physics Faculty, Vilnius University.
Address: Saulėtekio al. 9, 10222 Vilnius, Lithuania.

Summary of the thesis was distributed on March 19, 2012.
The thesis is available for review at the libraries of Vilnius University and Centre for Physical Sciences and Technology.

VILNIAUS UNIVERSITETAS

FTMC FIZIKOS INSTITUTAS

Paulius Každailis

**NUOTĖKIO AKUSTINĖS BANGOS AKUSTOOPTINĖJE IR
AKUSTOELEKTRINĖJE SĄVEIKOJE**

Daktaro disertacijos santrauka

Fiziniai mokslai, fizika (02 P)

Vilnius, 2012

Disertacija rengta 2006-2011 metais Vilniaus universitete.

Mokslinis vadovas:
- Prof. habil. dr. Daumantas Čiplys (Vilniaus universitetas, fiziniai mokslai, fizika – 02 P)

Konsultantas:
- Doc. dr. Romualdas Rimeika (Vilniaus universitetas, fiziniai mokslai, fizika – 02 P)

Disertacija ginama Vilniaus universiteto fizikos mokslo krypties taryboje:

Pirmininkas:
- Prof. habil. dr. Gintautas Tamulaitis (Vilniaus universitetas, fiziniai mokslai, fizika – 02 P);

Nariai:
- Prof. habil. dr. Alfonsas Grigonis (Kauno technologijos universitetas, fiziniai mokslai, fizika – 02 P);
- Dr. Rimantas Miškinis (Fizinių ir technologijos mokslų centro Puslaidininkių fizikos institutas, fiziniai mokslai, fizika – 02 P).
- Prof. dr. Šarūnas Paulikas (Vilniaus Gedimino technikos universitetas, technologijos mokslai, elektros ir elektronikos inžinerija – 01 T);
- Doc. dr. Vytautas Samulionis (Vilniaus universitetas, fiziniai mokslai, fizika – 02 P);

Oponentai:
- Prof. habil. dr. Rymantas Kažys (Kauno technologijos universitetas, technologijos mokslai, elektros ir elektronikos inžinerija – 01 T);
- Doc. dr. Vytautas Kunigėlis (Vilniaus universitetas, fiziniai mokslai, fizika – 02 P).

Disertacija bus ginama viešame Fizikos mokslo krypties tarybos posėdyje 2012 m. balandžio 20 d. 15 val., Vilniaus universitete, Fizikos fakultete, 815 auditorijoje.
Adresas: Saulėtekio al. 9, 10222 Vilnius, Lietuva.

Disertacijos santrauka išsiuntinėta 2012 m. kovo 19 d.
Disertaciją galima peržiūrėti Vilniaus universiteto bei Fizinių ir technologijos mokslų centro bibliotekose.

INTRODUCTION

Relevance of the work

The interaction of acoustic waves and light, called the acousto-optic (AO) interaction, provides an efficient tool for probing the acoustic wave properties not only at a crystal surface but also at any point within the substrate bulk. This is very important in a design of bulk acoustic wave devices for various applications. For example, the acoustic bulk-wave radiation into a solid from leaky surface acoustic waves (SAWs) excited by interdigital transducers (IDTs) on the solid surface has been successfully employed for sensing purposes in chemical, biological and medical applications [1]. ZX-$LiNbO_3$ (lithium niobate) and YX-$LiTaO_3$ (lithium tantalate) substrates, which support leaky surface modes with a strong bulk-wave radiation [2], [3], are frequently used for such sensors [4–6]. The experimental studies of the IDT-radiated bulk wave properties have been mostly performed by tracking the wave at the substrate surface [7], [8]. Meanwhile, there have been a few investigations of AO diffraction by IDT-generated bulk waves [9–11], but not of the diffraction due to the radiation from leaky SAWs.

On the other hand, the AO interaction enables an efficient control of light parameters. Bulk wave AO devices have found numerous applications as light modulators, deflectors, tunable filters [10], [12–28]. For example, recent achievements in image processing revealed the importance of the AO devices for biomedical and diagnostic applications [29]. For excitation of acoustic waves in such devices, a thin piezoelectric plate/film is bonded/deposited onto a device edge. These techniques are rather complicated and not fully compatible with the planar technologies of electronics manufacturing. With the advent of SAW technologies, the IDTs found wide applications due to their versatility, comparatively simple fabrication and planar technology. However, the diffraction of free propagating light by conventional Rayleigh SAWs is less efficient compared to that for the bulk acoustic waves because of considerably smaller interaction length. In this PhD thesis, the experimental investigation and theoretical model of anisotropic light diffraction by bulk acoustic waves radiated by an IDT and excited at the leaky SAW resonance in ZX-$LiNbO_3$ and YX-$LiTaO_3$ crystals are reported. This type of interaction allows for combining benefits of the IDT technology with the enhanced interaction length and efficiency of bulk-wave-type interaction.

Mixed-valence perovskite manganites were studied intensively in recent years mainly due to the observed paramagnetic (PM) to ferromagnetic (FM) transition at Curie temperature T_c ($T_c \cong 100 \div 390$ K), the colossal magnetoresistance effect, a variety of other unique electric, magnetic, structural properties and their potential for various applications [30–39]. The presence of strong Jahn-Teller electron-phonon coupling in the manganites suggests that the acoustic technique might be an effective tool for investigations of these materials [30], [40], [41]. The important information about electric, magnetic, structural manganite properties and their interrelation can be obtained by such investigations. Unique properties of manganites offer new possibilities for design of various electronic and magnetoelectronic (spintronic) devices [33], [40], [42]. In this PhD thesis, the experimental investigation of leaky-SAW-radiated bulk wave propagation in thin film $La_{0.67}Sr_{0.33}MnO_3$ – $LiNbO_3$ and $La_{0.67}Sr_{0.33}MnO_3$ – $LiTaO_3$ structures is reported, and the theoretical model of acoustic wave interaction with a layered thin conductive film – piezoelectric substrate structure is applied to describe the experimental results.

The aim and tasks of the work

The aim of the thesis was to investigate the interaction of leaky acoustic waves with a free-propagating laser light and thin manganite films. For this purpose, the following tasks were set:

1) Perform modelling and parameter calculation of leaky acoustic wave propagation and its interaction with light in crystals and with thin manganite films, prepare a review of worldwide research on these topics.

2) Master the surface acoustic wave technology and fabricate interdigital transducers on lithium niobate and lithium tantalate crystals needed for experiments.

3) Experimentally investigate the propagation of leaky waves and their interaction with laser light in lithium niobate and lithium tantalate crystals.

4) Experimentally investigate the influence of $La_{0.67}Sr_{0.33}MnO_3$ film on Rayleigh wave propagation in lithium niobate crystals.

5) Experimentally investigate the influence of $La_{0.67}Sr_{0.33}MnO_3$ film on leaky wave propagation in lithium tantalate crystal.

Scientific novelty

1) The acousto-optic diffraction by leaky surface acoustic wave radiation into a crystal bulk has been investigated for the first time.

2) The new method of acousto-optic light polarization control by leaky acoustic waves has been demonstrated.

3) The parameters of leaky acoustic wave radiation were obtained by acousto-optic probing.

4) The impact of $La_{0.67}Sr_{0.33}MnO_3$ film on Rayleigh and leaky acoustic waves has been observed and explained.

Research result approbation and publications

The results obtained and discussed in this work have been published in 10 scientific articles and presented in 10 scientific conferences. One more article is accepted for publication in *Microwave and Optical Technology Letters* journal and one is submitted to *Ultrasonics* journal.

Thesis content

PhD thesis consists of introduction, literature review, experimental technique description, presentation of results and discussion, conclusions, and reference list. The reference list consists of 218 entries. There are 174 pages including 104 figures and 14 tables in the thesis.

Statements presented for defence

1) Interdigital transducers deposited on the surface of piezoelectric crystals of certain configurations efficiently excite leaky surface acoustic waves, which radiates energy into crystal bulk in the form of directional bulk-wave beam.

2) The anisotropic light diffraction by radiation from leaky waves takes place in lithium niobate and lithium tantalate crystals. This new type AO interaction is more efficient than that employing Rayleigh waves and, at the same time, more compatible with today's planar electronics technologies than the diffraction by "conventional" bulk waves.

3) By means of AO technique the main leaky surface wave radiation parameters

(radiation angle, beam width, propagation velocity, intensity variation) are obtained.

4) Light diffraction by leaky wave radiation is promising in the design of the new AO devices, e.g. light polarization controllers.

5) Leaky wave radiated acoustic beam can be employed for probing the properties of thin semiconductor films formed on the piezoelectric crystal surface. Due to the acousto-electric (AE) interaction the reflection of this beam from $LiTaO_3$ crystal surface coated with $La_{0.67}Sr_{0.33}MnO_3$ film depends on the film conductance which varies with temperature.

LITERATURE REVIEW

The Rayleigh and leaky surface acoustic wave propagation in piezoelectrics is examined, the evolution history of acousto-optics, principles of AO interaction, various AO devices, investigations employing optical probing of the acoustic wave properties are overlooked in the 2nd chapter. Furthermore, the review of perovskite manganites and their interaction with acoustic waves is presented. The pictures and graphs are given in the source original language and notations in the literature review.

EXPERIMENTAL TECHNIQUE

The 3rd chapter is intended for the description of the properties and layout of used test samples ZX-$LiNbO_3$, YX-$LiTaO_3$, structures $La_{0.67}Sr_{0.33}MnO_3$ thin film – YZ-$LiNbO_3$, $La_{0.67}Sr_{0.33}MnO_3$ thin film – YX-$LiTaO_3$. The IDT S-parameter measurements (using vector network analyzer) and calculations, acousto-optic and acousto-electric measurement techniques are also presented in this chapter. The leaky SAW radiation into the crystal bulk was excited by applying modulated RF generator signal to the IDT. Anisotropic diffraction of He-Ne laser light (632.8 nm) by leaky acoustic wave radiation in ZX-$LiNbO_3$ and YX-$LiTaO_3$ crystals was monitored by means of measuring diffracted beam intensity with the photomultiplier tube (PMT), while the incidence and diffraction angles were read out using goniometer scale. The manganite ($La_{0.67}Sr_{0.33}MnO_3$) thin films DC magnetron sputtered on the surface of YZ-$LiNbO_3$ and YX-$LiTaO_3$ crystals were subjected to the interaction with Rayleigh waves and leaky wave radiation from the IDT, respectively. The transmitted wave amplitude and phase were measured at

receiving IDT using vector network analyzer and film sheet resistance was obtained from the external voltage drop on the load resistor connected in series. For the temperature measurements the samples were placed into cryostat with liquid nitrogen and internal heater.

RESULTS AND DISCUSSION

In the 4th chapter, the properties of bulk waves radiated by an IDT at leaky SAW resonance (leaky SAW radiation) are analyzed, also experimental results and calculations based on theoretical models concerning acoustic wave interaction with free propagating laser light in ZX-LiNbO$_3$, YX-LiTaO$_3$ crystals and with thin manganite films in structures La$_{0.67}$Sr$_{0.33}$MnO$_3$ − YZ-LiNbO$_3$, La$_{0.67}$Sr$_{0.33}$MnO$_3$ − YX-LiTaO$_3$ are discussed.

The leaky waves in ZX-LiNbO$_3$ and YX-LiTaO$_3$ substrates are strongly damped because of the energy radiation into the crystal bulk in the form of a slow shear bulk wave, the velocity of which along the crystal surface is lower than that of the leaky wave. The phase-matching condition

$$V_L \cos\alpha = V_B(\alpha) \tag{1}$$

determines the radiated wave propagation angle α with respect to the crystal surface. Here $V_B(\alpha)$ is the direction-dependent bulk wave velocity. Taking the literature [43], [44] leaky SAW velocity values (which are close to the experimental ones) in free (V_L=4517 m/s) and metallised (V_L=4389 m/s) ZX-LiNbO$_3$ surfaces, in accordance with equation (1), the slow shear bulk wave propagation angles α=26^0 and α=22^0 corresponding to the bulk wave velocities V_B=4561 m/s and V_B=4570 m/s, respectively, are obtained. Experimental leaky SAW velocity value V_L=3975 m/s in YX-LiTaO$_3$ crystal corresponds to the bulk wave propagation angle α=27.6^0 and bulk wave velocity V_B=3522 m/s. These values are in good agreement with literature data [3], [45].

AO diffraction in anisotropic crystals takes place with light polarization rotation [46], i.e. in case of ordinary polarized incident light the diffracted beam is of extraordinary polarization. The interacting light and acoustic wave vectors satisfy the momentum conservation condition [46]:

$$\vec{k}_k \pm \vec{K}_a = \vec{k}_d, \tag{2}$$

where $\vec{k}_k$ and $\vec{k}_d$ are the wave vectors of incident and diffracted light, respectively, $\vec{K}_a$ – acoustic wave vector. Acoustic and light wave vector diagram in ZX-LiNbO$_3$ crystal is depicted in Fig. 1., where $\vec{k}_o$ and $\vec{k}_e$ are the wave vectors of ordinary and extraordinary polarized light, respectively. For a given direction and modulus of acoustic wave vector, there are two possible configurations (*a* and *b)* of optical wave vectors allowing for the conversion of the ordinary wave to an extraordinary one and vice versa.
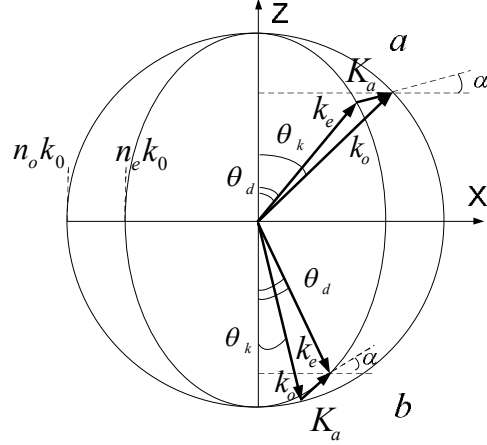

Fig. 1. Wave vector diagram of AO diffraction in ZX-LiNbO$_3$ crystal. Incident light is ordinary polarized.

For the case of the ordinary incident wave, Eq. 2 can be expressed in the form:

$$n_o \sin \theta_k \pm \frac{f \lambda_0}{V(\alpha)} \cos \alpha = n_e(\theta_d) \sin \theta_d \ , \tag{3}$$

$$n_o \cos \theta_k \mp \frac{f \lambda_0}{V(\alpha)} \sin \alpha = n_e(\theta_d) \cos \theta_d \ , \tag{4}$$

where the angles $\theta_{k,d}$ determine the directions of incident and diffracted beams inside the crystal (with respect to the Z and Y axis in LiNbO$_3$ and LiTaO$_3$, respectively), while f is acoustic frequency and λ_0 is light wavelength. The direction dependent (dependent in ZX plane of LiNbO$_3$ and independent in YX plane of LiTaO$_3$) refractive index of the diffracted wave is

$$n_e(\theta_d) = \left(\frac{\cos^2 \theta_d}{n_o^2} + \frac{\sin^2 \theta_d}{n_e^2} \right)^{-1/2} , \tag{5}$$

where n_o and n_e are the ordinary and extraordinary refractive indices of the crystal. By solving the Eq. system (3) and (4) with respect to $\theta_{k,d}$ and applying the Snell's law, the
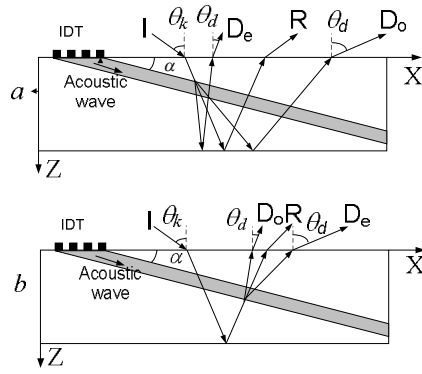
Fig. 2. Light and acoustic wave propagation in ZX-LiNbO$_3$ sample. Incident light diffracts on its way from the crystal upper surface to the bulk (*a*) or reflected from the bottom surface (*b*). I – incident randomly polarized, R – reflected, D$_o$ and D$_e$ – diffracted ordinary and extraordinary light, respectively. θ_k and θ_d – incidence and diffraction angles, respectively, α – bulk wave propagation angle with respect to the crystal surface.

angles determining the directions of incident and diffracted light beams outside the crystal in accordance with acoustic wave propagation angle, velocity and frequency can be evaluated. The interacting light and acoustic wave propagation in optically negative ($n_o > n_e$) LiNbO$_3$ crystal is depicted in Fig. 2*a* and *b*. These cases correspond to the wave vector diagram configurations shown in Fig. 1*a* and *b*, respectively. Laser light is incident at LiNbO$_3$ XY surface and ZX is the diffraction plane. Incident randomly polarized light in the crystal splits into ordinary and extraordinary beams which overlap due to a comparatively small difference between their refractions indices. However, after diffraction (with polarization rotation) at the acoustic beam the directions of ordinary and extraordinary light differ sufficiently allowing the beams to be distinguished in space and separately detected. In one case (Fig. 2*a*), the light diffracts at acoustic beam on its way from the crystal upper surface to the bulk, then two beams with mutually orthogonal polarizations reflect from the crystal bottom surface and are detected with the PMT. In the other case (Fig. 2*b*), the incident light reflects from the crystal bottom surface and only then diffracts at acoustic beam. In case *a*, the extraordinary polarized diffracted light comes out of the crystal at a smaller angle and the ordinary polarized diffracted light – at a larger angle than the incidence angle. In case *b*, the ordinary polarized diffracted light comes out of the crystal at a smaller angle and the extraordinary polarized diffracted light – at a larger angle than the incidence angle.

When ordinary or extraordinary polarized light is incident, in each of the above discussed cases (Fig. 2*a* and *b*), instead of two diffracted beams there will be only one orthogonally polarized to the incident light.
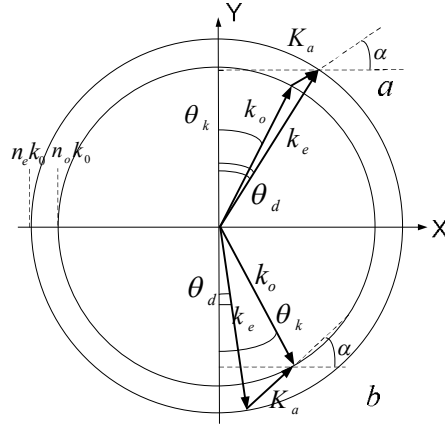

Fig. 3. Wave vector diagram of AO diffraction in YX-LiTaO$_3$ crystal. Incident light is ordinary polarized.
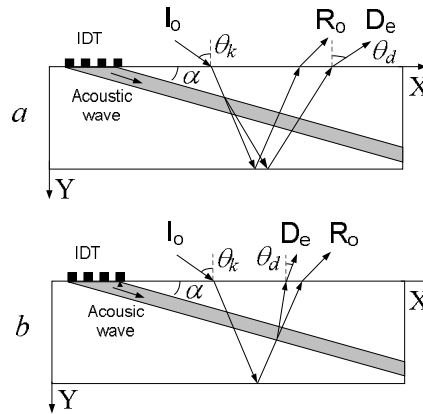

Fig. 4. Light and acoustic wave propagation in YX-LiTaO$_3$ sample. Incident light diffracts on its way from the crystal upper surface to the bulk (*a*) or reflected from the bottom surface (*b*). I$_o$ – incident ordinary, R – reflected, D$_e$ – diffracted extraordinary light. θ_k and θ_d – incidence and diffraction angles, respectively, α – bulk wave propagation angle with respect to the crystal surface.

In accordance with the wave vector diagram (Fig. 3.) and using Eq. system (3) and (4), one can calculate light incidence and diffraction angles for the AO diffraction in YX-LiTaO$_3$ crystal. In contrast to LiNbO$_3$ case, LiTaO$_3$ is an optically positive crystal, i.e. its extraordinary light refractive index is larger than the ordinary one $n_e>n_o$, and both indices are direction independent in the crystal YX plane. In case of ordinary polarized

incident light and given leaky wave radiation (bulk wave) propagation direction the two AO interaction wave vector configurations (Fig. 3.*a* and *b*) were investigated: diffracted (at acoustic beam) extraordinary light is obtained on its way from the crystal upper surface to the bulk (*a* – corresponds to Fig. 4.*a*) or reflected from the crystal bottom surface (*b* – corresponds to Fig. 4.*b*). In case *a,* the extraordinary light diffracts at a larger and, in case *b* – at the smaller angle than the incidence angle. Light and acoustic wave propagation in the YX plane of LiTaO$_3$ is depicted in Fig. 4.

The relative diffracted light intensity dependencies on ordinary and extraordinary light incidence angle in ZX-LiNbO$_3$ for various leaky acoustic wave frequencies and wave vector configurations are shown in Fig. 5.*a* and *b*. The measurements were performed with 120 μm, 60 μm, 50 μm, 40 μm, and 24 μm period IDTs (Table 1). For every IDT (leaky wave frequency) the peak of the diffracted light intensity is observed at a certain light incidence angle satisfying the momentum conservation condition. One can see that for various acoustic frequencies, incident light polarizations and AO interaction wave vector diagram configurations the momentum conservation condition is satisfied at different light incidence angles which increase with acoustic frequency. The relative diffracted light intensity dependencies on the ordinary light incidence angle in YX-LiTaO$_3$ for various leaky acoustic wave frequencies and wave vector configurations are shown in Fig. 6. The measurements were performed with 120 μm, 60 μm, 50 μm, 40 μm, and 32 μm period IDTs (Table 1). AO interaction takes place with light polarization rotation, thus, in case of ordinary incident light the diffracted beam bears extraordinary polarization. As can be seen in Fig. 6, for various acoustic frequencies and AO interaction wave vector diagram configurations the momentum conservation condition is satisfied at different light incidence angles.

Table 1. Experimental IDT and leaky SAW parameters.

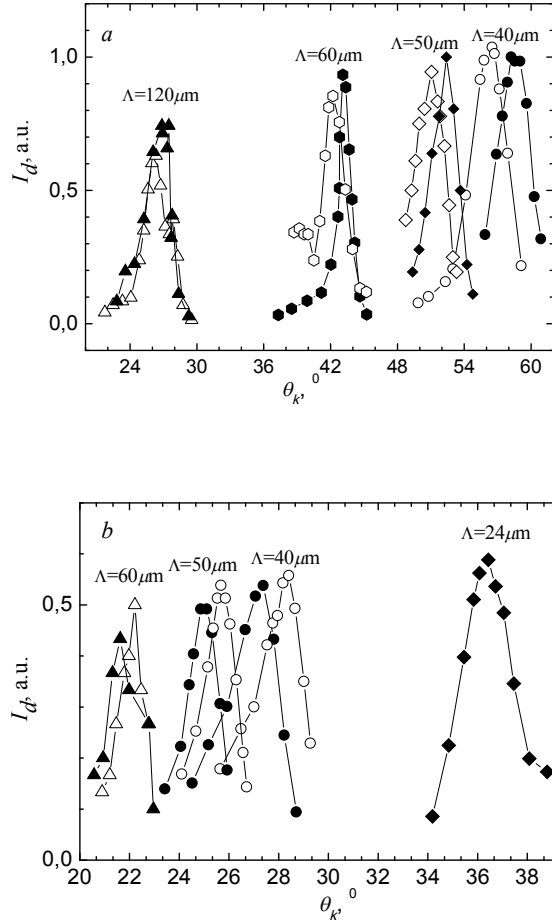| IDT		#1	#2	#3	#4	#5	#6
Period Λ_L, μm		120	60	50	40	32	24
Number of periods		15	15	35	20	15	40
Aperture, mm		1.3	1.3	1.3	1.3	1.3	1.3
LiNbO$_3$	Center frequency f_0, MHz	36.0	71.4	87.4	110.0	-	187.6
	Leaky SAW velocity, m/s	4320	4284	4370	4400	-	4502
LiTaO$_3$	Center frequency f_0, MHz	32.7	66.9	79.5	97.8	124.9	-
	Leaky SAW velocity, m/s	3924	4014	3975	3912	3997	-

Fig. 5. The relative diffracted light intensity dependencies on polarized light incidence angle for various leaky SAW frequencies in LiNbO$_3$ (*a* and *b* correspond to configuration of Fig. 1.*a* and *b*, respectively). Full dots denote ordinary incident and extraordinary diffracted, empty dots – extraordinary incident and ordinary diffracted light.
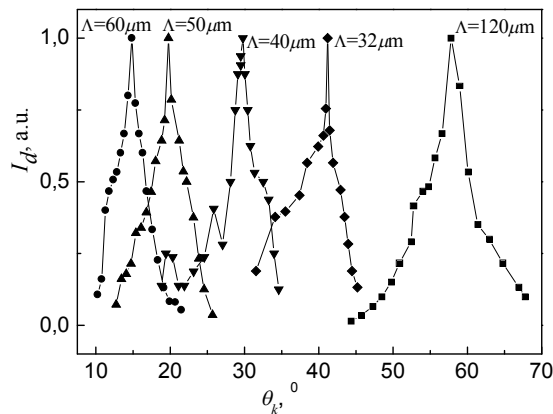

Fig. 6. The relative extraordinary diffracted light intensity dependencies on ordinary light incidence angle for various leaky SAW frequencies in LiNbO$_3$ (120 μm IDTs correspond to configuration of Fig. 3*a* and Fig. 4*a*, other IDTs – to Fig. 3*b* and Fig. 4*b*).

We have measured the light incidence angles θ_k at which the AO diffraction takes place in the leaky SAW frequency range from 36 MHz to 187 MHz. The experimental dependencies of the ordinary light incidence angle corresponding to the diffracted light intensity maximum on acoustic frequency in ZX-LiNbO$_3$ for wave vector configurations of Fig. 1a and b are shown in Fig. 7a and b, respectively. The light incidence angle increase with acoustic frequency. The measurement results are in good agreement with calculations using Eqs. (3) and (4). In calculations, we used these ZX-LiNbO$_3$ refractive index values: n_o=2.286, n_e=2.2 [47], [48]. Leaky SAW radiated bulk wave propagation angle α and velocity V_B were chosen as fitting parameters. The best agreement between experimental and calculation results was obtained at α=25^0 and $V_{B=}$4050 m/s. These values, in turn, meet well the literature data [43], [44] and calculations using Eq. (1).
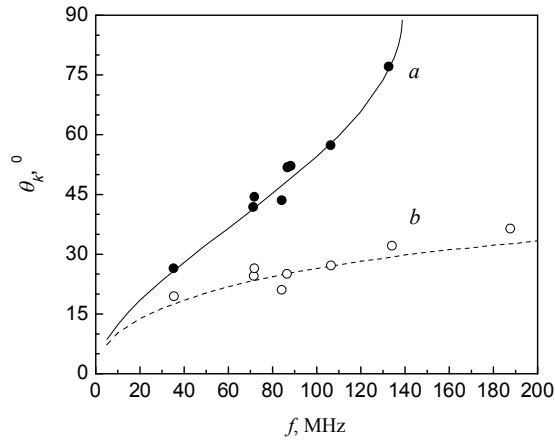

Fig. 7. Dependencies of the ordinary light incidence angle corresponding to the diffracted light intensity maximum on leaky SAW frequency in ZX-LiNbO$_3$ (a and b correspond to the wave vector configurations of Fig. 1.a and b, respectively. Dots – experiment, lines – calculations using V_B=4050 m/s, α=25^0.

In YX-LiTaO$_3$, for both wave vector configurations shown in Fig. 3a and b, the measured dependencies of the ordinary light incidence angle corresponding to the diffracted light intensity maximum on acoustic frequency are depicted in Fig. 8a and b, respectively. The experimental dependencies of $\theta_k(f)$ are compared to the calculated ones. In the calculations, we used refractive index values n_o=2.175, n_e=2.18 [47], [48]. The acoustic radiation angle α and velocity V_B were taken as fitting parameters. The best fit of calculated and measured dependencies, shown in Fig. 8a and b, is obtained with

$\alpha=31^0$, V_B =3530 m/s and $\alpha=35^0$, V_B =3509 m/s, respectively. These values are in good agreement with literature data [3], [45]. In accordance with the wave vector diagram of Fig. 3*a* and *b*, momentum conservation condition satisfying light incidence angle respectively decreases with increasing acoustic frequency in case of Fig. 8*a* and increases in case of Fig. 8*b*.
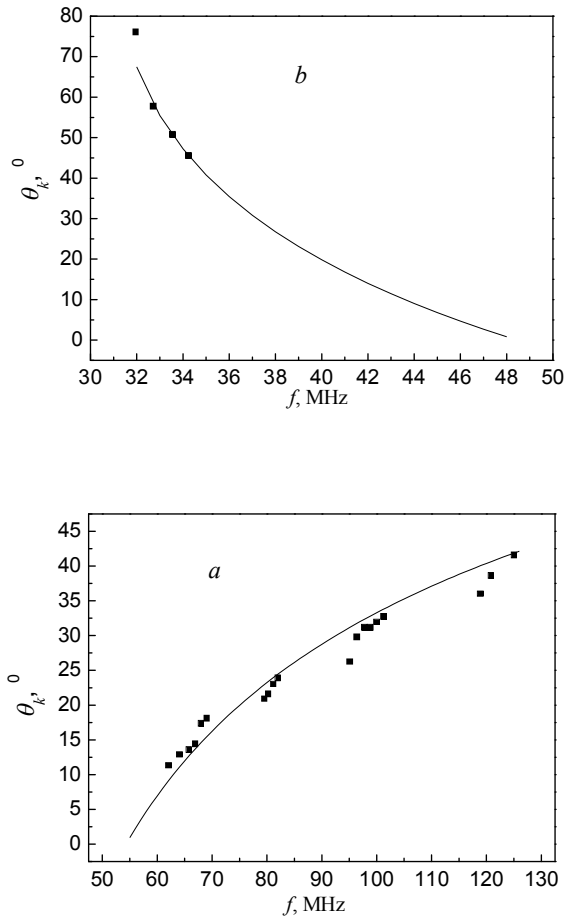

Fig. 8. Dependencies of the ordinary light incidence angle corresponding to the diffracted light intensity maximum on leaky SAW frequency in YX-LiTaO$_3$ (*a* and *b* correspond to wave vector configuration Fig. 3*a* and *b*, respectively). Dots – experiment, lines – calculations with $\alpha=35^0$, V_B =3509 m/s (*a*) and $\alpha=31^0$, V_B =3530 m/s (*b*).

In order to compare the efficiency of light diffraction by Rayleigh and leaky waves the diffracted light intensity dependence on the voltage applied to the IDT in ZX-LiNbO$_3$ sample was measured (Fig. 9). The intensity of light (diffraction efficiency) diffracted by leaky wave radiation is considerably higher as compared to the diffraction by Rayleigh waves.
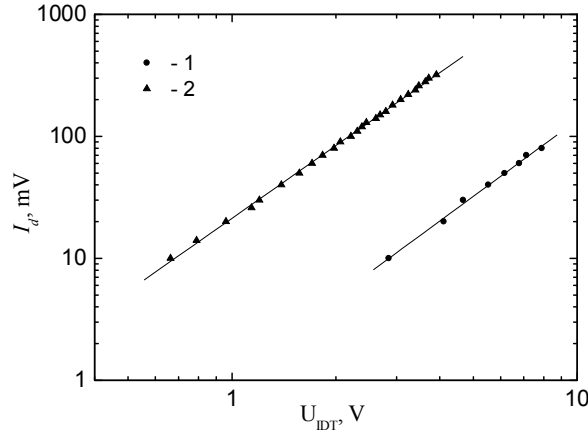
Fig. 9. Diffracted light intensity dependence on the voltage applied to the IDT in ZX-LiNbO$_3$ sample. Rayleigh wave – curve 1, f=75.6 MHz; leaky wave radiation – curve 2, f=87.4 MHz.

Light diffraction by acoustic waves is an effective and versatile tool for optical radiation control. Here we present approach combining the advantages of IDT technology and more efficient (compared to Rayleigh waves) AO diffraction of free propagating light by leaky SAW radiation in ZX-LiNbO$_3$.
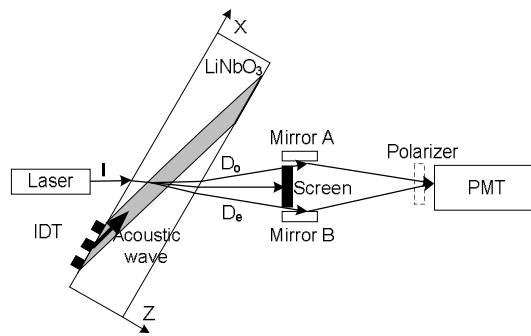

Fig. 10. Experimental setup for the light polarization control in ZX-LiNbO$_3$. I – randomly polarized incident light, D_o and D_e – ordinary and extraordinary polarized diffracted light, respectively.

The experimental setup and vector diagram of interacting light and acoustic waves are shown in Fig. 10 and Fig. 11, respectively. When randomly polarized light is incident at the crystal surface it splits into two beams with mutually orthogonal polarizations. Due to the small difference in refractive indices, these beams overlap before reaching the acoustic wave (angular separation only 8′ at the incidence angle 58^0). However,

17

directions of the diffracted beams of both polarizations differ sufficiently (2.7^0) allowing the beams to be distinguished in space and separately detected. With the help of mirrors A and B (Fig. 10) the two diffracted beams are directed to the PMT. The light polarization could be analyzed using a glass polarizing filter. The response time of the given setup is determined mostly by the speed of acoustic wave in the crystal and doesn't exceed 1 μs.
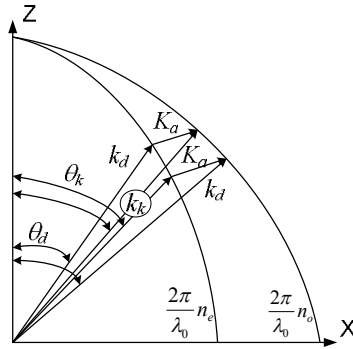

Fig. 11. AO interaction wave vector diagram in ZX-LiNbO$_3$.

The dependencies of diffracted light intensity on acoustic frequency at the constant incidence angle of randomly polarized light are shown in Fig. 12. Both diffracted beams with orthogonal polarizations were directed to the input of PMT, as shown in Fig. 10, and measurements were performed for each beam separately by blocking one of them. The polarization of diffracted light is ordinary for curve *a* and extraordinary for curve *b* of Fig. 12. As seen, the relative intensities of beams with orthogonal polarizations can be varied by changing the acoustic frequency. At different frequencies, the momentum conservation condition is satisfied for different directions within the angular spreading of the acoustic beam. Therefore, the shape of diffracted light intensity dependencies on frequency is determined by both the frequency response of the IDT and the angular profile of acoustic beam intensity. Finally, the both diffracted beams were superposed with the help of mirrors A and B as shown in Fig. 10. The PMT response to the superposition of the both beams is shown by curve *c* in Fig. 12. The polarization of light resulting from the beam superposition varies with frequency. For example, at 108 MHz the light is polarized in the XZ plane of the LiNbO$_3$ substrate (extraordinary beam), and at 112 MHz the light polarization is normal to the XZ plane (ordinary beam). Switching the frequency between these values allows for switching between two states of

polarization, while setting any frequency value within this range results in an arbitrary elliptic output light polarization. The initial polarization state with no preference in polarization direction is recovered by adding two beams at 110 MHz. The presented light polarization control method is purely electronic.
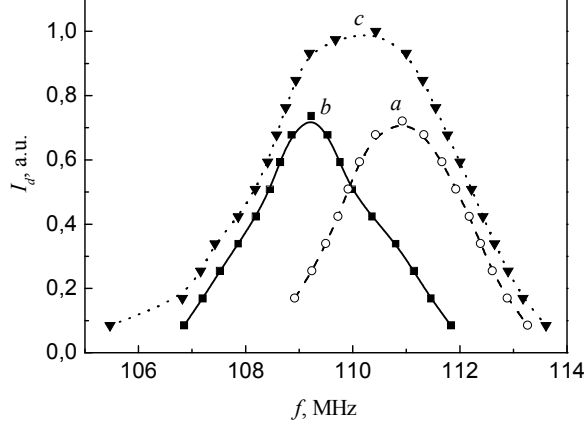

Fig. 12. Dependencies of diffracted light relative intensity on acoustic frequency at constant incidence angle 58° of randomly polarized light. Ordinary (*a*), extraordinary (*b*) beams and their superposition (*c*).

Further, let's discuss the interaction of the leaky SAW radiation into the YX-LiTaO$_3$ crystal bulk with thin manganite (La$_{0.67}$Sr$_{0.33}$MnO$_3$) films. Tape-like manganite films (area of 4 mm^2) with thickness 120 nm were DC-magnetron sputtered (at 500^{0}C) onto a polished Y-surface of single crystal LiTaO$_3$ substrates in the region where the acoustic wave reflects from the surface. Before reaching the receiving IDT, the leaky wave radiation reflects from the bottom, the top (region covered with manganite film) and again from the bottom crystal surfaces. In the region of overlapping incident and reflected acoustic beams near the surface, the inhomogeneous wave that travels with the speed of the leaky SAW along the surface and decays with depth is created [49]. Acoustic wave attenuation due to AE interaction with La$_{0.67}$Sr$_{0.33}$MnO$_3$ film is expressed by [50]:

$$A = 8.686 \frac{2\pi}{\Lambda} \frac{K^2}{2} \frac{R_m / R_s}{1 + (R_m / R_s)^2} \quad \text{(dB/m)}, \tag{6}$$

here K^2 is the electromechanical coupling constant of the substrate, $R_m = 1/[\varepsilon_0(\varepsilon + 1)V]$, ε_0 is the dielectric permittivity of vacuum, ε is the effective relative dielectric constant of

the structure, Λ is the acoustic wavelength, and V is the leaky wave velocity.

The decrease of manganite sheet resistance of the both used samples #4 and #5 on YX-LiTaO$_3$ with increasing temperature indicates paramagnetic isolator state (shown in Fig. 13a and Fig. 14a, respectively). The relatively high resistance values and the absence of the PM-FM transition in the film may be attributed to a number of anti-structural defects and reduced density of carriers [34], [35], [51–59] [3,4,16-24] due to a relatively low growth temperature.

Experimental and calculated (using measured La$_{0.67}$Sr$_{0.33}$MnO$_3$ sheet resistance values) leaky wave attenuation temperature dependencies in samples #4 (leaky SAW f=22.2 MHz) and #5 (leaky SAW f=66.9 MHz) are depicted in Fig. 13b and Fig. 14b, respectively. The attenuation maxima values (corresponding to the manganite sheet resistance value R_s~200 kΩ) increase with acoustic frequency and meet well the theoretical calculations (from Eq. (6)). On the other hand, the acoustic attenuation maxima are shifted to the higher temperature range as compared to the calculations. In case of free LiTaO$_3$ crystal (without manganite film), the acoustic attenuation remains constant within the whole measured temperature range (Fig. 13b and Fig. 14b).
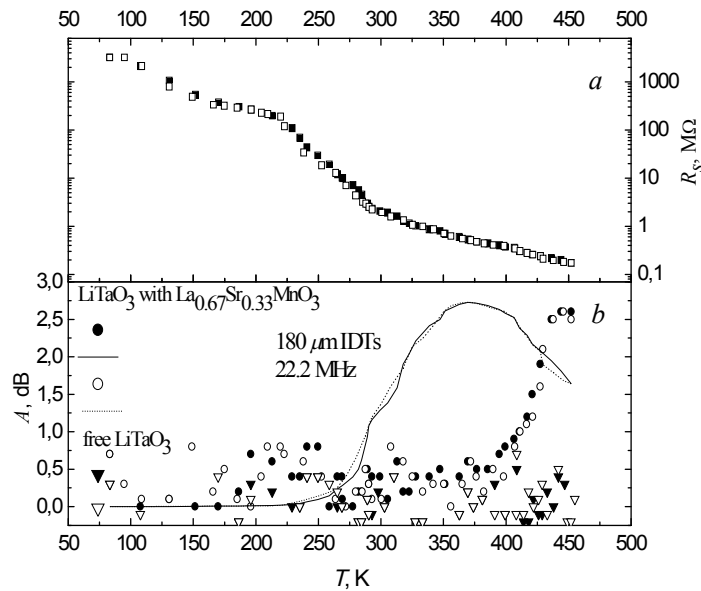

Fig. 13. La$_{0.67}$Sr$_{0.33}$MnO$_3$ sheet resistance (a) and leaky acoustic wave attenuation (b) dependencies on temperature in sample #4. Full dots – experiment in heating mode, empty dots – experiment in cooling mode, solid line – calculations in heating mode, dashed line – calculations in cooling mode.

Fig. 14. $La_{0.67}Sr_{0.33}MnO_3$ sheet resistance (*a*) and leaky acoustic wave attenuation (*b*) dependencies on temperature in sample #5. Full dots – experiment in heating mode, empty dots – experiment in cooling mode, solid line – calculations in heating mode, dashed line – calculations in cooling mode.
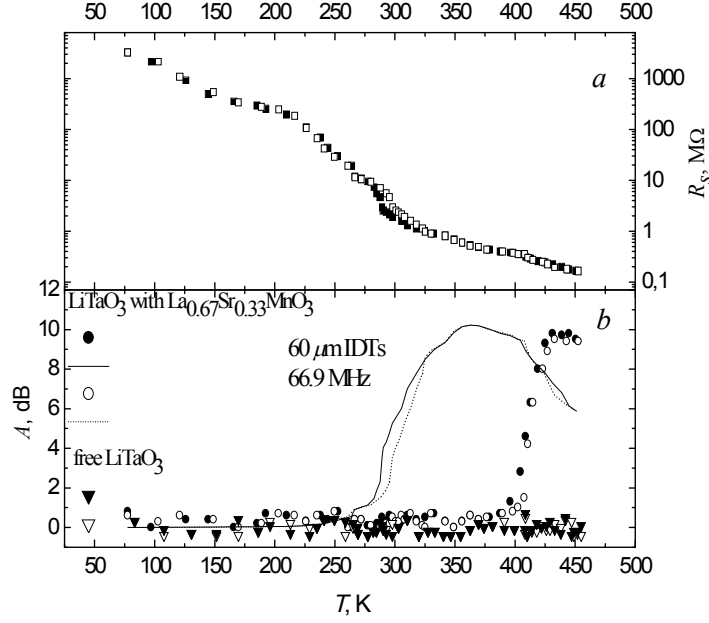
Experimental and calculated temperature dependencies of transmitted leaky wave phase in $LiTaO_3$ with manganite film (curves 2) and without it (curves 1) for samples #4 (leaky SAW *f*=22.2 MHz) and #5 (leaky SAW *f*=66.9 MHz) are shown in Fig. 15 and Fig. 16, respectively. As seen, the leaky wave phase decreases with increasing temperature. The distinction of the curves for samples with and without manganite film becomes noticeable at temperatures above 370 K. To explain the observed leaky wave phase-versus-temperature behaviour, we consider the AE interaction effect on the acoustic wave propagation velocity [50]. When sheet resistance of the film on a piezoelectric substrate changes from infinity to the finite value R_s, the corresponding velocity change is:

$$\frac{\Delta V_{AE}}{V} = -\frac{K^2}{2}\frac{(R_m/R_s)^2}{1+(R_m/R_s)^2}. \tag{7}$$

The velocity change leads to the change in the transmitted wave phase, which can be expressed in degrees as:

21

$$\Delta\Phi_{AE} = 360\frac{l}{\Lambda}\frac{\Delta V_{AE}}{V}, \tag{8}$$

where l is the IDT length (corresponding to AE interaction length under the manganite film, 0.72 mm and 0.9 mm for samples #4 and #5, respectively). The transmitted wave phase also varies with temperature due to the acoustic velocity variation (ΔV_{SUB}) caused by the temperature dependence of the substrate elastic constants, and due to the change in the IDT spacing, ΔL, caused by the thermal expansion:

$$\Delta\Phi_{SUB} = 360\frac{L}{\Lambda}\left(\frac{\Delta V_{SUB}}{V} - \frac{\Delta L}{L}\right). \tag{9}$$

The phase variation in the free-surface sample (curves 1, Fig. 15.*a* and Fig. 16.*a*) is approximated by the linear function (curves 1, Fig. 15.*b* and Fig. 16.*b*). The total phase dependence in the sample with manganite film (curves 2, Fig. 15.*b* ir Fig. 16.*b*) is obtained by adding the AE term calculated from Eqs. (7) and (8) using the measured sheet resistance values. The calculated leaky wave phase-versus-temperature dependencies in samples #4 and #5 are close the experimental ones, but the measurement accuracy is not sufficient to unambiguously evaluate manganite film influence on acoustic wave velocity and phase.
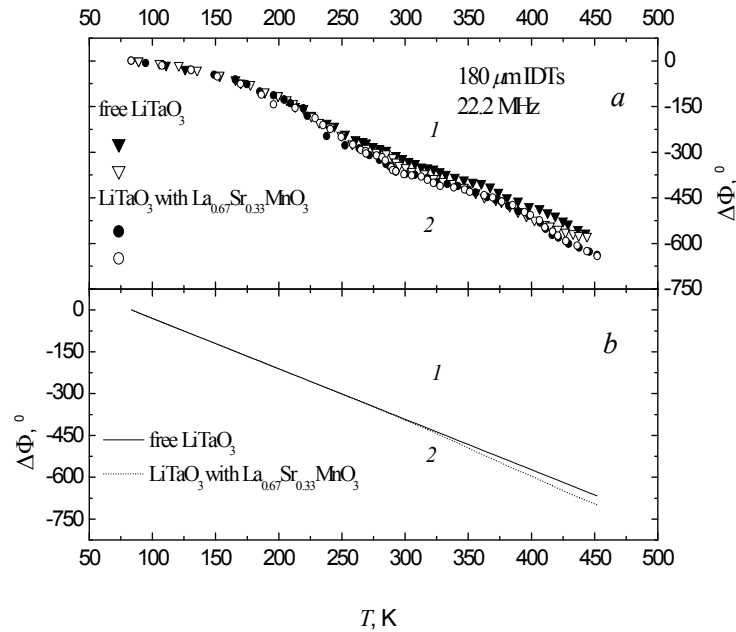

Fig. 15. Leaky wave radiation transmitted phase temperature dependencies in sample #4, *a* – experiment, *b* – calculation. Full dots – experiment in heating mode, empty dots – experiment in cooling mode.
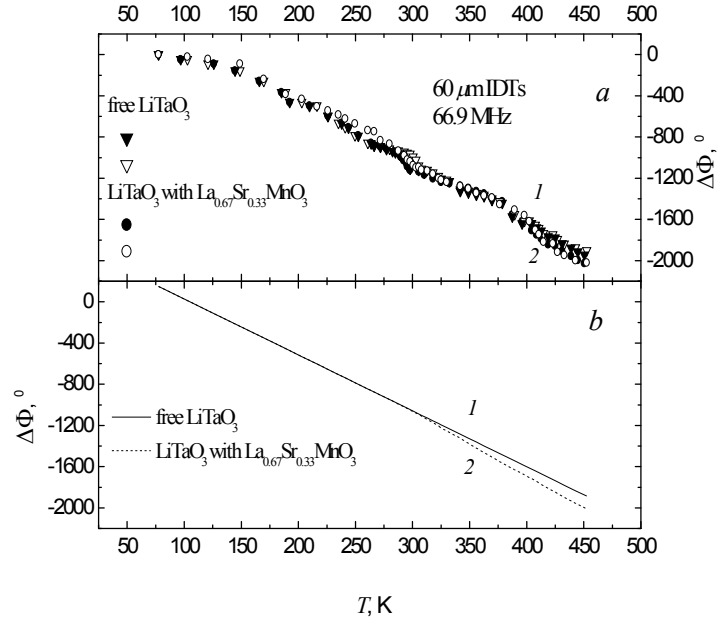
Fig. 16. Leaky wave radiation transmitted phase temperature dependencies in sample #5, a – experiment, b – calculation. Full dots – experiment in heating mode, empty dots – experiment in cooling mode.

Finally, let's outline some important remarks on the investigated AE interaction. The leaky wave radiation propagates at an angle into YX-LiTaO$_3$ bulk and interacts with manganite film located in the region where the wave reflects from the crystal surface. In our measurements, the manganite film was located on the same crystal surface as the IDTs, however, this experimentally demonstrated interaction is analogous to the case when the film and IDTs are on the opposite crystal surfaces. The latter configuration is attractive in various applications, especially for aggressive environment sensors, etc., where IDTs must be protected from possible damage by means of separating the sensing (surface coated with film) and generating (IDTs) parts. Furthermore, due to its prevailing shear horizontal (parallel to crystal surface) polarization leaky wave is subjected to less attenuation when in contact with liquids and other materials [29].

CONCLUSIONS

- The experimental results of laser light diffraction by leaky surface acoustic wave radiation into the crystal bulk (the dependencies of light incidence angle corresponding to the diffracted light intensity maximum on the leaky wave

frequency in LiNbO$_3$ and LiTaO$_3$) are in good agreement with the calculations in accordance with theoretical anisotropic acousto-optic diffraction model based on wave vector diagrams. Acoustic wave propagation angle and velocity values in LiNbO$_3$ and LiTaO$_3$ crystals were obtained from the best fit of measurement and calculation results. These values meet well the data published in literature.

- The beam width, intensity variation of the leaky surface wave radiation into the crystal bulk were obtained and efficiency of the light diffraction by leaky wave radiation and Rayleigh waves was compared using the acousto-optic technique. The efficiency of light diffraction by leaky wave radiation is considerably higher than that of diffraction by Rayleigh waves.

- The demonstrated light polarization control by leaky surface wave radiation into the crystal bulk is purely electronic. This technology may be employed in dynamic light polarization control devices.

- The interaction of leaky surface acoustic wave radiation into the crystal bulk with thin manganite films in structure La$_{0.67}$Sr$_{0.33}$MnO$_3$ film – YX-LiTaO$_3$ was experimentally investigated in a wide temperature range and acousto-electric contribution to the acoustic wave attenuation was measured. This attenuation value meets well the calculation results based on the theoretical model of acoustic wave propagation in structure thin conductive film – piezoelectric substrate.

- The leaky wave suitability for light control and investigations of thin manganite film properties was experimentally demonstrated. The measurement results are well justified by theoretical models/calculations. The interdigital transducer technology advantages were incorporated with higher efficiency of light diffraction by bulk waves (compared to Rayleigh waves). While probing thin manganite (or other) films by leaky wave radiation, the generating part can be protected from possible damage by placing transducers in the opposite crystal side with respect to the sensitive surface (coated with film).

REFERENCE LIST

[1]   J. C. Andle and J. F. Vetelino, "Acoustic wave biosensors," *Proceedings of the IEEE Ultrasonics Symposium*, pp. 451–460, 1995.

[2]   K. Yamanouchi and K. Shibayama, "Propagation and amplification of Rayleigh

waves and piezoelectric leaky surface waves in LiNbO$_3$," *Applied Physics Letters*, vol. 43, pp. 856–862, 1970.

[3]   K. Yamanouchi and M. Takeuchi, "Applications for piezoelectric leaky surface waves," *Proceedings of the IEEE Ultrasonics Symposium*, pp. 11–18, 1990.

[4]   F. Jose, D. T. Haworth, U. R. Kelkar, Z. A. Shana, "LiNbO$_3$ acoustic plate mode sensor for dilute ionic solutions," *Electronics Letters*, vol. 26, no. 13, pp. 834–835, 1990.

[5]   J. C. Andle, J. F. Vetelino, M. W. Lade and D. J. McAllister, "An acoustic plate mode biosensor," *Sensors and Actuators B*, vol. 8, no. 2, pp. 191–198, 1992.

[6]   J. Renken, R. Dahint and M. Grunze, "Multifrequency evaluation of different immunosensors on acoustic plate mode sensors," *Analytical Chemistry*, vol. 68, pp. 176–182, 1996.

[7]   S. Jen and C. S. Hartmann, "Laser probe Investigation of leaky surface waves on 41 and 64-LiNbO$_3$," *Proceedings of the IEEE Ultrasonics Symposium*, vol. 293, pp. 293–296, 1994.

[8]   J. V. Knuuttila, J. J. Vartiainen, J. Koskela, V. P. Plessky, C. S. Hartmann, M. M. Salomaa, "Bulk-acoustic waves radiated from low-loss surface-acoustic-wave resonators," *Applied Physics Letters*, vol. 84, no. 9, pp. 1579–1581, 2004.

[9]   W. S. Goruk, G. I. Stegeman, "Acousto-optic measurement of bulk wave generation by interdigital transducers excited at SAW resonance," *Journal of Applied Physics*, vol. 50, no. 11, pp. 6729–6732, 1979.

[10] K. Y. Hashimoto, M. Yamaguchi, and H. Kogo, "Optic-spectrum analyzer using DBAW acousto-optic deflector," *Proceedings of the IEEE Ultrasonics Symposium*, pp. 361–366, 1984.

[11] L. Palmieri, G. Socino, E. Verona, "Acoustic beam steering by an interdigital transducer for wideband bulk wave acoustooptic deflectors," *Proceedings of the IEEE Ultrasonics Symposium*, p. 358–261, 1985.

[12] L. Bei, G. I. Dennis, H. M. Miller, T. W. Spaine, J. W. Carnahan, "Acousto-optic tunable filters: fundamentals and applications as applied to chemical analysis techniques," *Progress in Quantum Electronics*, vol. 28, pp. 67–87, 2004.

[13] E.S. Wachman, W.-H. Niu, D.L. Farkas, "Imaging acousto-optic tunable filter with 0.35-micrometer spatial resolution," *Applied Optics*, vol. 35, pp. 5220–5226, 1996.

[14] I. C. Chang, "Noncollinear acousto-optic filter with large angular aperture,"

Applied Physics Letters, vol. 25, no. 7, pp. 370–372, 1974.

[15]   D. R. Suhre, E. Villa, "Imaging spectroradiometer for the 8–12-vm region with a 3-cm^{-1} passband acousto-optic tunable filter," *Applied Optics*, vol. 37, no. 12, pp. 2340–2345, 1998.

[16]   N. Gupta, R. Dahmani, S. Choy, "Acousto-optic tunable filter based visible-to-near-infrared spectropolarimetric imager," *Optical Engineering*, vol. 41, pp. 1033–1038, 2002.

[17]   J. Romier, J. Selves, J. Gastelluetchegorry, "Imaging spectrometer based on an acousto-optic tunable filter," *Review of Scientific Instruments*, vol. 69, no. 8, pp. 2859 – 2867, 1998.

[18]   S. R. Goldstein, L.H. Kidder, T.M. Herne, I.W. Levin, E.N. Lewis, "The design and implementation of a high-fidelity Raman imaging microscope," *Journal of Microscopy*, vol. 184, pp. 35–45, 1996.

[19]   A. D. Campiglia, D. M. Hueber, F. Moreau, and T. Vo-Dinh, "Phosphorescence imaging system using AOTF and charge coupled device," *Analytical Chimica Acta*, vol. 346, pp. 361–372, 1997.

[20]   H. T. Skinner, T. F. Cooney, S. K. Sharma and S. M. Angel, "Remote Raman micro-imaging using AOTF and a spatially coherent microfiber optical probe," *Applied Spectroscopy*, vol. 50, pp. 1007–1014, 1996.

[21]   A. D. Campiglia, F. Moreau, D.M. Hueber, T. Vo-Dinh, "Phosphorescence imaging system using an acousto-optic filter-based charge coupled device," *Analytica Chimica Acta*, vol. 351, pp. 229–239, 1997.

[22]   P. J. Treado, I. W. Levin, E. N. Lewis, "Indium antimonide (InSb) focal plane array (FPA) detection for near-infrared imaging microscopy," *Applied Spectroscopy*, vol. 48, pp. 607–615, 1994.

[23]   D. A. Glenar, J. J. Hillman, M. Lelouarn, R. Q. Fugate, J. D. Drummond, "Multispectral imagery of Jupiter and Saturn using adaptive optics and acousto-optic imaging," *Publications of the Astronomical Society of the Pacific*, vol. 109, pp. 326–337, 1997.

[24]   N. J. Chanover, D. A. Glenar, J. J. Hillman, "Multispectral near-IR imaging of Venus nightside cloud features," *Journal of Geophysical Research-Planets*, vol. 103, no. E13, pp. 31335–31348, 1998.

[25] K. M. Nield, A. Bittar, J. D. Hamlin, "Development of an all-sky-scanning spectroradiometer with a visible diode array and a near-infrared acousto-optic tunable filter," *Applied Optics*, vol. 36, pp. 7939–7947, 1997.

[26] O. Khait, S. Smirnov, C. D. Tran, "Multispectral imaging microscope with millisecond time resolution," *Analytical Chemistry*, vol. 73, pp. 732–739, 2001.

[27] Y. Inoue, J. Penuelas, "An AOTF-based hyperspectral imaging system for field use in ecophysiological and agricultural applications," *International Journal of Remote Sensing*, vol. 22, pp. 3883–3888, 2001.

[28] D. R. Suhre, J.G. Theordore, "White-light imaging by use of a multiple passband acousto-optic tunable filter," *Applied Optics*, vol. 35, no. 22, pp. 4494–4501, 1996.

[29] V. S. Chivukula, M. S. Shur, and D. Čiplys, "Recent advances in application of acoustic, acousto-optic and photoacoustic methods in biology and medicine," *Physica Status Solidi A*, vol. 204, no. 10, pp. 3209–3236, 2007.

[30] A. J. Millis, P. B. Littlewood, and B. I. Shraiman, "Double exchange alone does not explain the resistivity of $La_{1-x}Sr_xMnO_3$," *Physical Review Letters*, vol. 74, pp. 5144–5147, 1995.

[31] Y. Ilisavskii, A. Goltsev, K. Dyakonov, V. Popov, E. Yakhkind, V. P. Dyakonov, P. Gierłowski, A. Klimov, S. J. Lewandowski, and H. Szymczak, "Anomalous acoustoelectric effect in $La_{0.67}Ca_{0.33}MnO_3$ films," *Physical Review Letters*, vol. 87, p. 146602–05, 2001.

[32] J. J. Neumeier, M. F. Hundley, J. D. Thompson, and R. H. Heffner, "Substantial pressure effects on the electrical resistivity and ferromagnetic transition temperature of $La_{1-x}Ca_xMnO_3$," *Physical Review B*, vol. 52, p. R7006–R7009, 1995.

[33] J. Devenson, "Įvairialyčių lantano manganitų sandūrų gaminimas ir tyrimas," PhD Thesis, Vilnius University, Vilnius, 2009.

[34] A. Urushibara, Y Moritomo, T. Arima, A. Asamitsu, G. Kidoa, and Y. Tokura, "Insulator-metal transition and giant magnetoresistance in $La_{1-x}Sr_xMnO_3$," *Physical Review B*, vol. 51, no. 20, pp. 14103–14109, 1995.

[35] Y. Okimoto, T. Katsufuji, T. Ishikawa, T. Arima, and Y. Tokura, "Variation of electronic structure in $La_{1-x}Sr_xMnO_3$ f($0 \leqslant x \leqslant 0.3$) as investigated by optical conductivity spectra," *Physical Review Letters*, vol. 55, no. 7, pp. 4206–4214, 1997.

[36] N. Okawa, H. Tanaka, R. Akiyama, T. Matsumoto, T. Kawai, "Effects of film

thickness on surface flatness and physical properties in $La_{1-x}Sr_xMnO_3$ thin films investigated by scanning tunneling microscopy," *Solid State Communications*, vol. 114, pp. 601–605, 2000.

[37] Y. Z. Chen, J. R. Sun, A. D. Wei, W. M. Lu, S. Liang, and B. G. Shen, "Charge ordering transition near the interface of the (011)-oriented $La_{1-x}Ca_xMnO_3$ (x-1/8) films," *Applied Physics Letters*, vol. 93, p. 152515–1–3, 2005.

[38] C. Zhu and R. Zheng, "Elastic-moduli and ultrasonic-attenuation anomalies near antiferromagnetic phase transitions in $La_{1-x}Ca_xMnO_3$," *Journal of Applied Physics*, vol. 87, pp. 3579–3581, 2000.

[39] Y. Ilisavskii, A. Goltsev, K. Dyakonov, V. Popov, E. Yakhkind, V.P. Dyakonov, P. Gierlowski, A. Klimov, S. J. Lewandowski, H. Szymczak, "Acoustic and acoustoelectric studies of manganite films," *Journal of Magnetism and Magnetic Materials*, vol. 242–245, pp. 707–709, 2002.

[40] J. M. D. Coey, M. Viret, S. Molnar, "Mixed-valence manganites," *Advances in Physics*, vol. 48, no. 2, pp. 167–193, 1999.

[41] J. M. D. Coey, M. Viret, L. Ranno, and K. Ounadjela, "Electron localization in mixed - valency manganites," *Physical Review Letters*, vol. 75, no. 21, p. 3910, 1995.

[42] P. LeClair, J.K. Ha, H.J.M Swagten, J.T. Kohlhepp, C.H. van de Vin, W.J.M. de Jonge, "Large magnetoresistance using hybrid spin filter devices," *Applied Physics Letters*, vol. 80, p. 625, 2002.

[43] P. H. Carr, "The generation and propagation of acoustic surface Waves at microwave frequencies," *IEEE Transactions on Microwave Theory and Techniques*, vol. 17, no. 1, pp. 845–855, 1969.

[44] P. H. Carr, "New low loss high coupling mode up to 1 GHz on $LiNb0_3$," *Proceedings of the IEEE Ultrasonics Symposium*, pp. 679–682, 1977.

[45] K. Nakamura, M. Kazumi, and H. Shimizu, "SH-type and Rayleigh-type surface waves on rotated Y-cut $LiTaO_3$," *Proceedings of the IEEE Ultrasonics Symposium*, pp. 819–822, 1977.

[46] A. Yariv, P.Yeh, *Optical waves in crystals*. New York: Wiley, 1984.

[47] D. Royer, E. Dieulesaint, *Elastic Waves in Solids II*. Paris: Springer, 1999.

[48] В. В. Леманов, О. В. Шакин, "Рассеяние света на упругих волнах в одноосных кристаппах," *ФТТ*, vol. 14, pp. 229–236, 1972.

[49] R. Rimeika, A. Sereika, and D. Čiplys, "Acoustoelectric effects in reflection of leaky acoustic waves from $LiTaO_3$ crystal surface coated with metal film," *Applied Physics Letters*, vol. 98, p. 052909–1–3, 2011.

[50] K. A. Ingebrigtsen, "Linear and nonlinear attenuation of acoustic surface waves in a piezoelectric coated with a semiconducting film," *Journal of Applied Physics*, vol. 41, pp. 454–459, 1970.

[51] S. Fang, Z. Pang, F. Wang, L. Lin and S. Han, "Annealing effect on transport and magnetic properties of $La_{0.67}Sr_{0.33}MnO_3$ thin films grown on glass substrates by RF magnetron sputtering," *Journal of Materials Sciences and Technology*, vol. 27, no. 3, pp. 223–226, 2011.

[52] L. Signorini, M. Riva, M. Cantoni, R. Bertacco, F. Ciccacci, "Epitaxial $La_{2/3}Sr_{1/3}MnO_3$ thin films with unconventional magnetic and electric properties near the Curie temperature," *Thin Solid Films*, vol. 515, no. 2006, pp. 496–499.

[53] S.Y. Yang, W.L. Kuang, Y. Liou, W.S. Tse, S.F. Lee, Y.D. Yao, "Growth and characterization of $La_{0.7}Sr_{0.3}MnO_3$ films on various substrates," *Journal of Magnetism and Magnetic Materials*, vol. 268, pp. 326–331, 2004.

[54] D. R. Sahu, D. K. Mishrab, J.-L. Huanga, B. K. Roul, "Annealing effect on the properties of $La_{0.7}Sr_{0.3}MnO_3$ thin film grown on Si substrates by DC sputtering," *Physica B*, vol. 396, pp. 75–80, 2007.

[55] D. R. Sahu, "Lateral parameter variations on the properties of $La_{0.7}Sr_{0.3}MnO_3$ films prepared on Si (1 0 0) substrates by dc magnetron sputtering," *Journal of Alloys and Compounds*, vol. 503, pp. 163–169, 2010.

[56] I. Bergenti, V. Dediu, M. Cavallini, E. Arisi, A. Riminucci, C. Taliani, "Properties of thin manganite films grown on semiconducting substrates for spintronics applications," *Current Applied Physics*, vol. 7, pp. 47–50, 2007.

[57] X. Zhu, H. Shen, Z. Tang, K. Tsukamoto, T. Yanagisawa, M. Okutomi, N. Higuchi, "Structural and magnetotransport properties of $La_{0.67}Sr_{0.33}MnO_3$ thin films prepared by metal–organic decomposition under different annealing process," *Journal of Alloys and Compounds*, vol. 488, pp. 437–441, 2009.

[58] C. S. Xiong, Z. L. Luo, Y. H. Xiong, G. N. Meng, Z. P. Jian, W. Yi, D. G. Zong, Z. C. Xia, S. L. Yuan, "The effect of oxygen partial pressure on the electron–magnetic properties of $La_{0.67}Sr_{0.33}MnO_{3-d}$ epitaxial films with different orientations," *Journal of*

Magnetism and Magnetic Materials, vol. 257, pp. 369–376, 2003.

[59] M. C. Terzzoli, D. Rubi, S. Duhalde, M. Villafuerte, M. Sirena, L. Steren, "Transport properties of pulsed laser deposited $La_{0.67}Sr_{0.33}MnO_3$ thin films," *Applied Surface Science*, vol. 186, pp. 458–462, 2002.

LIST OF PUBLICATIONS ON SUBJECT OF THE THESIS

1) P. Každailis, R. Giriūnienė, R. Rimeika, D. Čiplys, K. Šliužienė, V. Lisauskas, B. Vengalis, and M. S. Shur, "Surface acoustic wave propagation in lanthanum-strontium manganese oxide-lithium niobate structures" – submitted to „*Ultrasonics*" journal.

2) T. Gertus, M. Mikutis, P. Kazdailis, R. Rimeika, D. Ciplys and V. Smilgevicius, "Surface-acoustic-wave phononic crystal device fabricated by femtosecond laser ablation" – accepted for publication in "*Microwave and Optical Technology Letters*" journal.

3) P. Každailis, R. Giriūnienė, R. Rimeika, D. Čiplys, "Application of leaky surface acoustic waves for investigation of thin-film properties," *Proceedings of the ICSV 18: 18th International Congress of Sound and Vibration*, Rio de Janeiro, 2011, pp. 413-421.

4) R. Rimeika, P. Každailis, D. Čiplys, S. Balakauskas, "Control of light polarization by acousto-optic diffraction from leaky acoustic wave in $LiNbO_3$," *Optics Letters*, vol. 36, no. 13, pp. 2581-2583, 2011.

5) T. Gertus, P. Každailis, R. Rimeika, D. Čiplys and, V. Smilgevičius, "Surface acoustic wave transducers fabricated by femtosecond laser ablation," *Electronics Letters*, vol. 46, no. 17, pp. 1175 - 1176, 2010.

6) R. Giriūnienė P. Každailis, D. Čiplys, K. Šliužienė, B. Vengalis, V. Lisauskas, "Acoustoelectric interaction in thin lanthanum manganite films," *Proceedings of the Conference Radiation Interaction with Material and Its Use in Technologies*, Kaunas, 2010, pp. 185-188.

7) P. Každailis, R. Rimeika and D. Čiplys, "Analysis of the leaky surface acoustic wave radiation in YX-$LiTaO_3$ for symmetric and non-symmetric IDTs," *Proceedings of the IEEE Ultrasonics Symposium*, Rome, 2009, pp. 2049-2052.

8) P. Každailis, R. Rimeika, D. Čiplys, "Light interaction with leaky acoustic wave

radiation in YX-LiTaO$_3$," *Proceedings of the Conference Acoustics'08*, Paris, 2008, pp. 2085 - 2089.

9) P. Každailis, R. Rimeika, D. Čiplys, "Optical probing of IDT-excited bulk acoustic wave radiation pattern in YX-LiTaO$_3$," *Proceedings of the Conference Actuality and Perspectives of Natural Science*, Šiauliai, 2008, pp. 171-175.

10) P. Každailis, R. Rimeika, D. Čiplys, and M. S. Shur, "Light diffraction by IDT-radiated bulk acoustic waves in ZX-LiNbO$_3$," *Proceedings of the 2007 IEEE Ultrasonics Symposium*, New York, 2007, pp. 2323-2326.

11) R. Rimeika, D. Čiplys, P. Každailis, and M. S. Shur, "Anisotropic acousto-optic diffraction by leaky wave radiation in ZX-LiNbO$_3$," *Applied Physics Letters*, vol. 90, pp. 181935 (1-3), 2007.

12) R. Gaska, M. S. Shur, Q. Fareed, P. Každailis, D. Čiplys, R. Rimeika, A. Sereika, "Dependence of AlGaN-based SAW oscillator frequency on temperture," *Electronics Letters*, vol. 40, no. 10, pp. 637-639, 2004.

SHORT INFORMATION ABOUT THE AUTHOR

2000 - 2004 studied at Vilnius University Faculty of Physics and earned Bachelor's Degree in Electronic Engineering.

2004 - 2006 studied at Vilnius University Faculty of Physics and earned Master's Degree in Electronic Engineering.

2006 - 2011 PhD studies at Vilnius University (Physics science direction).

Contact: paulius.kazdailis@ff.stud.vu.lt

REZIUMĖ

Darbo aktualumas

Akustinių bangų ir šviesos – akustooptinė (AO) sąveika įgalina tirti akustinių bangų savybes ne tik kristalo paviršiuje, bet ir tūryje. Tai aktualu kuriant tūrinių bangų prietaisus įvairiems taikymams. Pavyzdžiui, sunertiniais plonasluoksniais keitikliais žadinamų nuotėkio paviršinių akustinių bangų (PAB) spinduliuotė į kristalo tūrį buvo sėkmingai pritaikyta jutikliuose chemijoje, biologijoje ir medicinoje [1]. Tokiuose jutikliuose dažnai naudojami ZX-LiNbO$_3$ (ličio niobato) ir YX-LiTaO$_3$ (ličio tantalato) kristalai [2–4], pasižymintys efektyvia nuotėkio bangų spinduliuote į kristalo tūrį [5],

[6]. Sunertinais keitikliais spinduliuojamų tūrinių akustinių bangų savybės eksperimentiškai dažniausiai nustatomos zonduojant bangą kristalo paviršiuje [7], [8]. Iki šiol yra atlikta keletas AO difrakcijos eksperimentų [9–11], kai sunertiniais keitikliais žadinamos tūrinės bangos, bet ne nuotėkio PAB spinduliuotė į tūrį. Kita vertus, AO sąveiką galima efektyviai panaudoti šviesos parametrų valdyme. Tūrinių bangų AO prietaisai – šviesos moduliatoriai, deflektoriai, derinami filtrai plačiai naudojami praktikoje [10], [12–28]. Pasiekimai atvaizdų apdorojime atskleidė AO įtaisų svarbą biomedicinos ir diagnostikos taikymams [29]. Akustinių bangų žadinimui tūriniuose AO prietaisuose prie jų krašto yra tvirtinama pjezoelektrinė plokštelė, tačiau ši technologija yra gana sudėtinga ir ne visiškai suderinama su šiuolaikinėmis plokštuminėmis elektronikos technologijomis. Tuo tarpu, sunertiniai PAB keitikliai yra plačiai naudojami dėl savo įvairiapusiškumo, sąlyginai paprasto gamybos proceso ir suderinamumo su plokštuminėmis technologijomis. Vis dėlto, lyginant su tūrinių bangų atveju, laisvai sklindančios šviesos difrakcijos „klasikinėmis" Reilėjaus bangomis efektyvumas yra mažesnis dėl ženkliai mažesnio sąveikos ilgio. Šioje disertacijoje pateikiami anizotropinės šviesos difrakcijos nuotėkio paviršinių akustinių bangų spinduliuote į kristalo tūrį ZX-LiNbO$_3$ ir YX-LiTaO$_3$ eksperimentiniai rezultatai ir teorinis modelis. Tokio tipo sąveika įgalina suderinti sunertinių keitiklių technologijos privalumus su didesniu šviesos sąveikos su tūrinėmis akustinėmis bangomis ilgiu ir efektyvumu.

Dėmesys mišraus valentingumo manganitams, turintiems perovskito kristalinę gardelę vis didėja dėl fazinio virsmo PM (paramagnetikas) – FM (feromagnetikas) Kiuri temperatūroje T_C (T_C~100÷390 K), milžiniškosios magnetovaržos (MMV) efekto, didelės unikalių tarpusavyje susijusių magnetinių, struktūrinių, elektrinių savybių įvairovės ir potencialo įvairiuose taikymuose [30–39]. Dėl stiprios Jahn-Teller tipo elektron-fononinės sąveikos akustiniai metodai yra įdomūs ir perspektyvūs tiriant manganitus [30], [40], [41]. Tokiuose tyrimuose gaunama svarbi informacija apie elektrines, magnetines, struktūrines manganitų savybes ir jų tarpusavio ryšį. Unikalios manganitų savybės atveria visiškai naujas galimybes įvairių elektronikos bei magnetoelektronikos (spintronikos) prietaisų kūrimui [33], [40], [42]. Šioje disertacijoje pateikiami nuotėkio paviršinių akustinių bangų spinduliuotės į tūrį sklidimo dariniuose La$_{0.67}$Sr$_{0.33}$MnO$_3$ plėvelė – LiNbO$_3$ ir La$_{0.67}$Sr$_{0.33}$MnO$_3$ plėvelė – LiTaO$_3$ eksperimentiniai rezultatai. Jiems aprašyti buvo pritaikytas akustinių bangų sklidimo sluoksniniame

darinyje laidi plėvelė – pjezoelektrikas teorinis modelis.

Disertacijos tikslas ir uždaviniai

Disertacinio darbo **tikslas** buvo ištirti nuotėkio akustinių bangų sąveiką su laisvai sklindančia lazerio šviesa bei plonais manganito sluoksniais. Tikslo įvykdymui buvo iškelti šie **uždaviniai**:

1) Atlikti nuotėkio akustinių bangų sklidimo, jų sąveikos su lazerio šviesa ir plonais manganito sluoksniais procesų modeliavimą, parametrų skaičiavimą, parengti pasaulyje atliktų tyrimų apžvalgą šiomis temomis.

2) Įsisavinti paviršinių akustinių bangų technologiją ir pagaminti tyrimams reikalingus keitiklius ant ličio niobato ir ličio tantalato kristalų.

3) Eksperimentiškai ištirti nuotėkio bangų sklidimą ir jų sąveiką su šviesa ličio niobato ir ličio tantalato kristaluose.

4) Eksperimentiškai ištirti $La_{0.67}Sr_{0.33}MnO_3$ sluoksnio įtaką Reilėjaus bangų sklidimui ličio niobato kristale.

5) Eksperimentiškai ištirti $La_{0.67}Sr_{0.33}MnO_3$ sluoksnio įtaką nuotėkio bangų sklidimui ličio tantalato kristale.

Rezultatų naujumas

1) Pirmą kartą ištirta akustooptinė difrakcija nuotėkio paviršinių akustinių bangų spinduliuote į kristalo tūrį.

2) Pademonstruotas laisvai sklindančios lazerio šviesos poliarizacijos ir kitų parametrų valdymas nuotėkio akustinėmis bangomis.

3) Akustooptinė metodika pritaikyta nuotėkio paviršinių akustinių bangų spinduliuotės į kristalo tūrį parametrų nustatymui.

4) Ištirta ir paaiškinta $La_{0.67}Sr_{0.33}MnO_3$ sluoksnio įtaka Reilėjaus ir nuotėkio bangoms.

Ginamieji teiginiai

1) Planariaisiais sunertiniais keitikliais, suformuotais ant pjezoelektrinių kristalų paviršiaus, žadinamos nuotėkio paviršinės bangos, kurių spinduliuotė suformuoja kryptingą tūrinių bangų pluoštelį.

2) Ličio niobato ir ličio tantalato kristaluose vyksta anizotropinė šviesos difrakcija nuotėkio bangų spinduliuojamu pluošteliu. Tai naujo tipo akustooptinė sąveika, efektyvesnė negu šviesos difrakcija Reilėjaus bangomis ir geriau suderinama su šiuolaikinėmis technologijomis negu difrakcija „klasikinėmis" tūrinėmis bangomis.

3) Akustooptiniu metodu nustatomi esminiai paviršinių nuotėkio bangų spinduliuotės parametrai (spinduliavimo kampas, pluoštelio plotis, sklidimo greitis, intensyvumo kitimas).

4) Šviesos difrakcija nuotėkio bangų spinduliuote yra perspektyvi taikymams kuriant naujus akustooptinius įtaisus, pav. šviesos poliarizacijos valdiklius.

5) Nuotėkio akustinių bangų spinduliuojamas pluoštelis gali būti naudojamas kaip zondas plonų puslaidininkinių sluoksnių, suformuotų ant pjezoelektrinio kristalo paviršiaus, savybėms tirti. Šio pluoštelio atspindys nuo $LiTaO_3$ kristalo paviršiaus, padengto manganito $La_{0.67}Sr_{0.33}MnO_3$ plėvele, dėl akustoelektrinės sąveikos priklauso nuo plėvelės laidumo, kintančio su temperatūra.

Išvados

- Lazerio šviesos difrakcijos nuotėkio paviršinių akustinių bangų spinduliuote į kristalo tūrį tyrimų rezultatai (šviesos kritimo kampo, atitinkančio difragavusios šviesos intensyvumo maksimumą, priklausomybės nuo nuotėkio bangų dažnio $LiNbO_3$ ir $LiTaO_3$ kristaluose) gerai sutampa su skaičiavimais, atliktais pagal teorinį anizotropinės akustooptinės difrakcijos modelį, paremtą banginių vektorių diagramomis. Iš geriausio matavimų ir skaičiavimų rezultatų sutapimo buvo rastos akustinių bangų sklidimo kampo ir greičio $LiNbO_3$ ir $LiTaO_3$ kristaluose vertės. Jos atitinka literatūroje pateiktus duomenis.

- Akustooptiniu metodu buvo nustatytas nuotėkio paviršinių bangų spinduliuotės į kristalo tūrį pluoštelio plotis, intensyvumo kitimas, o taip pat buvo palygintas šviesos difrakcijos nuotėkio bangų spinduliuote ir Reilėjaus bangomis efektyvumas. Difrakcija nuotėkio bangų spinduliuote į kristalo tūrį yra žymiai efektyvesnė nei Reilėjaus bangomis.

- Šviesos poliarizacijos valdymas nuotėkio paviršinių bangų spinduliuote į kristalo

tūrį atliekamas pilnai elektroniniu būdu. Ši technologija gali būti panaudota dinaminio šviesos poliarizacijos valdymo prietaisuose.

- Plačiame temperatūrų intervale eksperimentiškai ištyrus nuotėkio paviršinių bangų spinduliuotės į kristalo tūrį sąveiką su plonais manganitų sluoksniais darinyje $La_{0.67}Sr_{0.33}MnO_3$ plėvelė – $LiTaO_3$, buvo išmatuotas akustoelektrinės sąveikos indėlis į akustinių bangų slopinimą. Ši slopinimo vertė sutampa su skaičiavimų rezultatais, gautais remiantis akustinių bangų sklidimo sluoksniniame darinyje laidi plėvelė – pjezoelektrikas teoriniu modeliu.

- Eksperimentiškai buvo pademonstruotas nuotėkio bangų tinkamumas šviesos valdymui ir plonų manganito sluoksnių savybių tyrimui. Eksperimentų rezultatai yra gerai pagrįsti teoriniais modeliais/skaičiavimais. Sunertinių paviršinių bangų keitiklių technologijos privalumai buvo suderinti su didesniu šviesos difrakcijos tūrinėmis bangomis efektyvumu (lyginant su Reilėjaus bangomis). Zonduojant plonus manganitų (ir kitus) sluoksnius nuotėkio bangų spinduliuote, sunertinius keitiklius galima formuoti priešingoje kristalo pusėje jautriojo paviršiaus (padengto sluoksniu) atžvilgiu taip apsaugant generuojančiąją dalį nuo galimų pažeidimų.